Proceedings of ICRC 2001: 1703 © Copernicus Gesellschaft 2001

ICRC 2001

# AMS Antimatter Search Results

**M. Cristinziani for the AMS collaboration**

DPNC, Université de Genève, Switzerland

**Abstract.** A search for cosmic antinuclei by the Alpha Magnetic Spectrometer (AMS) is presented. The detector was flown on board space shuttle Discovery in June 1998 for 10 days on a $51.7^\circ$ orbit at altitudes $\sim 350$ km. Nuclei are identified by multiple energy loss and time-of-flight measurements and their rigidity is obtained by the bending inside the permanent magnet. $2.86 \times 10^6$ helium and $1.65 \times 10^5$ heavy nuclei have been precisely measured in a rigidity range $1 < R < 140$ GV, while no antinucleus at any rigidity were detected. Integrated upper limits on the flux ratio $\overline{Z}/Z$ are given which are independent on the incident spectrum.

## 1 Introduction

The existence (or absence) of antimatter nuclei in space is closely connected with the foundation of the theories of elementary particle physics, CP–violation, baryon number nonconservation, Grand Unified Theory (GUT), etc. Balloon–based cosmic ray searches for antinuclei at altitudes up to 40 km have been carried out for more than 20 years; all such searches have been negative (see e. g. Saeki et al. (1998)). The absence of annihilation gamma ray peaks excludes the presence of large quantities of antimatter within a distance of the order of 10 Mpc from the earth. The baryogenesis models are not yet supported by particle physics experimental data. To date baryon nonconservation and large levels of CP–violation have not been observed. The Alpha Magnetic Spectrometer (AMS) (Ahlen et al. , 1994) is scheduled for a high energy physics program on the International Space Station. A major objective of this program is to search for antinuclei using an accurate, large acceptance magnetic spectrometer. AMS was flown on the space shuttle *Discovery* on flight STS–91 in June 1998. This was primarily a test flight that would enable the AMS team to gather data on background sources, adjust operating parameters and verify the detector's performance under actual space flight conditions. A search for antimatter nuclei using the data collected during this precursor flight is reported. The signal investigated is nuclei with charge $Z \leq -2$ (see also Alcaraz et al. (1999))

*Correspondence to:* M. Cristinziani
(arkus.Cristinziani@physics.unige.ch)

## 2 AMS on STS–91

A schematic cross section in the bending plane of AMS as flown on STS–91 (Fig. 1) shows the permanent magnet, tracker, time of flight hodoscopes, Cerenkov counter and anticoincidence counters. The geometric acceptance was $\sim 0.3\,\mathrm{m}^2$sr. AMS as flown on STS–91 is described elsewhere (Viertel and Capell , 1998).

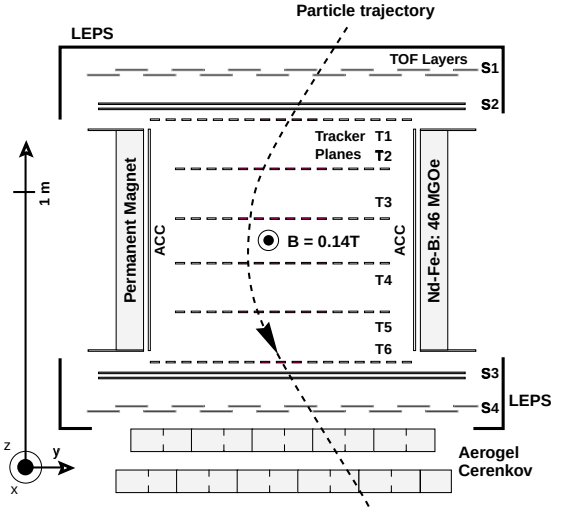


**Fig. 1.** Schematic view of AMS as flown on STS–91 (see text)

The cylindrical magnet was made out of a Nd-Fe-B alloy, providing an analyzing power, $BL^2$, of $0.14\,\mathrm{Tm}^2$. The trajectory of charged particles traversing the magnet bore was observed with a tracker made of six planes, T1 to T6, of double sided silicon microstrip detectors. For AMS on STS–91 only half of the tracker area was equipped. From the deflection the

rigidity, $\mathrm{R} = pc/|Z|e$ (GV), was measured. The tracker also provided a determination of charge magnitude, $|Z|$, through multiple energy loss measurements. Special care was taken to minimize the amount of material in the tracker construction; the total amount of material within the tracker volume was less than 3% of a radiation length parallel to the z–axis. During flight hits in the tracker were measured with an accuracy of $\sim 10\,\mu$m in the bending direction and $\sim 30\,\mu$m in the orthogonal directions. The resolution in terms of rigidity was verified for $|Z| \geq 2$ nuclei using helium and carbon ion beams at GSI–Darmstadt. At low momenta the resolution was limited by multiple scattering.

The particle direction and velocity were measured with a four layer, S1 to S4, time-of-flight (TOF) hodoscope. As shown in Fig. 1, two layers were above the magnet and two below. The paddles in each pair were orthogonal. The pulse height information recorded from the TOF paddles provided an additional determination of $|Z|$. The typical accuracy of the time of flight measurements was 105 psec for $|Z| = 2$.

The velocity measurement was complemented by a threshold Cerenkov counter made of aerogel with a refractive index of 1.035.

A layer of anticoincidence scintillation counters (ACC) covered the inner surface of the magnet to reject the background caused by particles passing through or interacting in the magnet walls and support structures. The detector was also shielded from low energy (up to several MeV) particles by thin carbon fiber walls (LEPS). For particles arriving from above, as shown in Fig. 1, the amount of material at normal incidence was $1.5\,\mathrm{g/cm^2}$ in front of the TOF system, and $3.5\,\mathrm{g/cm^2}$ in front of the tracker.

During flight the detector was located in the payload bay of the space shuttle and operated in vacuum. Events were triggered by the coincidence of signals in all four TOF planes consistent with the passage of a charged particle through the active tracker volume. Triggers with a coincident signal from the ACC were vetoed. A total of 100 million triggers were recorded.

After the flight, the detector was checked again. It was placed in a heavy ion (He, C) beam at GSI–Darmstadt at kinetic energies between 186 and 2000 MeV/nucleon at 600 different incident angles. It was then placed in a proton and pion beam at CERN with momentum from 2 to 14 GeV at 1200 different incident angles.

The continued monitoring of the detector confirmed that the detector performance before, during and after the flight remained the same. In particular, the alignment of the silicon tracker remained the same to an accuracy of $\sim 5\,\mu$m.

## 3 Event Reconstruction and Selection

After the shuttle had attained orbit, data collection commenced on 3 June 1998 and continued over the next nine days for a total of 184 hours. During data taking the shuttle altitude varied from 320 to 390 km and the latitude ranged between $\pm$ 51.7 degrees. Before rendezvous with the MIR space station the attitude of the shuttle was maintained to keep the z–axis of AMS (see Fig. 1) pointed within 45 degrees of the zenith. While docked, the attitude was constrained by MIR requirements and varied substantially. After undocking the pointing was maintained within 1, 20 and then 40 degrees of the zenith. Shortly before descent the shuttle turned over and the pointing was towards the nadir. For this search, data collected while passing through the South Atlantic Anomaly was excluded.

The procedure to search for antimatter began with event reconstruction, which included:

- Measurement of the particle rigidity, R, from the deflection of the trajectory measured by the tracker in the magnetic field. To ensure that the particle was well measured, hits in at least four tracker planes were required and the fitting was performed with two different algorithms, the results of which were required to agree.
- Measurement of the particle velocity, $\beta$, and direction, $\hat{z} = \pm 1$, from the TOF, where $\hat{z} = -1$ corresponds to a downward going particle (see Fig. 1).
- Determination of the magnitude of the particle charge, $|Z|$, from the measurements of energy losses in the tracker planes (corrected for $\beta$). For low charges, $|Z| \leq 2$ the additional information from the TOF scintillators was used.

The sign of the particle charge was derived from the deflection in the rigidity fit and the direction. The particle mass was derived from $|Z|\mathrm{R}$ and $\beta$.

The major backgrounds to the antimatter search ($Z \leq -2$) are the abundant amount of protons and electrons ($|Z| = 1$) and nuclei ($Z \geq +2$) with a poorly reconstructed trajectory. The detector response to $\mathrm{e}^-$, p, He and $Z$ was studied from data collected in flight, from the above mentioned GSI and CERN beam data and from Monte Carlo studies.

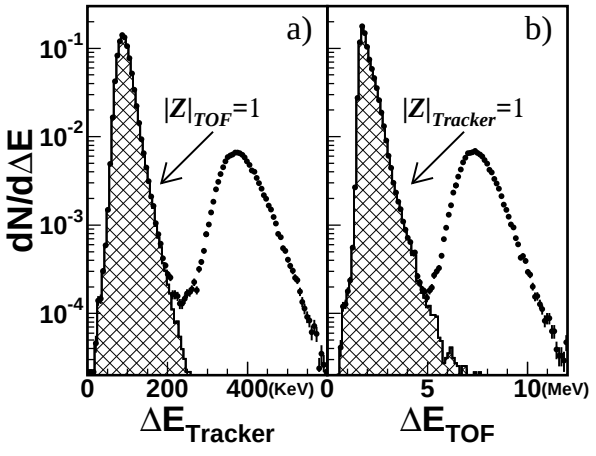


**Fig. 2.** Energy loss measurements (points) are made independently in the tracker (a) and TOF (b) for $|Z| \leq 2$ events. The hatched histogram shows which events were assigned to be $|Z| = 1$ by the other detector.

### 3.1 Selection of events with $|Z| \geq 2$

This was to ensure no contamination from $|Z| = 1$ events with a wrongly measured charge magnitude which would mimic $|Z| \geq 2$ events. Fig. 2 shows the energy deposition and the assigned charge magnitude as measured independently by the TOF and the tracker. The probability of the wrong charge magnitude being assigned by the combined TOF and tracker measurements was estimated to be less than $10^{-7}$.

### 3.2 Determination of the sign of the $|Z| \geq 2$ events

Key points of the background rejection procedure were the identification of:

(i) *Particle direction:* the sign of the charge is determined by the measurement of the particle direction. Due to the good time resolution, down- and upgoing particles are clearly distinguished. The direction was always correctly assigned.

(ii) *Large angle nuclear scattering events:* events in which a single nuclear scattering in one of the inner tracker planes, T2–T5, introduced a large angle kink in the track and might cause an incorrect measurement of the charge sign. This background was suppressed by a cut on the estimated rigidity error, and the requirement that the two rigidity values obtained by fitting the track using the first three and last three hits are in agreement.

(iii) *Events with collinear delta rays:* events with collinear debris, e. g. delta rays, from an interaction of the primary particle in the tracker material which may shift a measured point from the trajectory, leading to an incorrectly measured rigidity and charge sign. This background was efficiently rejected by an isolation cut which rejected events with an excess of energy observed in the vicinity of the track.

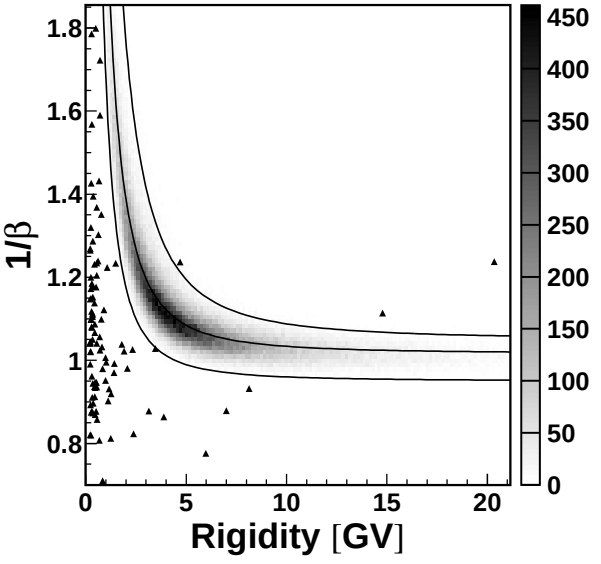


**Fig. 3.** Flight time versus rigidity for selected $Z > 2$ (histogram) and $Z < -2$ candidates (triangles). True $|Z| > 2$ should be concentrated around the central line. All antinuclei candidates are located outside the bands and are therefore rejected.

An additional cut ensuring the overall consistence of the velocity, rigidity and charge measurements is applied to the events passing all other quality cuts. Fig. 3 shows the distribution of $1/\beta$ versus rigidity together with the cuts applied for $|Z| > 2$ events. True $|Z| > 2$ events should be concentrated along the line $1/\beta = \sqrt{1 + (AM_n/ZR)^2}$, where A is the atomic number and $M_n$ the nucleon mass. Measurement errors in $\beta$, $Z$ or R cause scattering around this line. The shown cuts reject all remaining $Z < -2$ antimatter candidates and keep nearly all the $Z > 2$ events. A similar procedure is used in the case of $|Z| = 2$ events (see Alcaraz et al. (1999)).

## 4 Results and Interpretation

The result of our search is summarized in Fig. 4. We obtain a total of $2.86 \times 10^6$ He events and $1.65 \times 10^5$ $Z$ events up to a rigidity of 140 GV. We found no antimatter event at any rigidity.

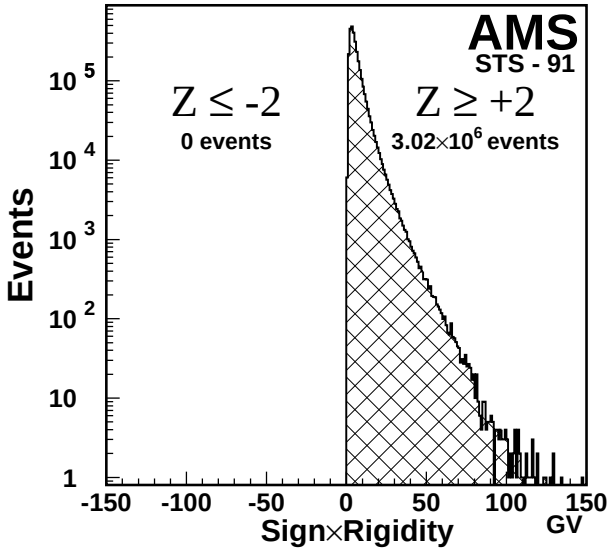


**Fig. 4.** Measured rigidity times the charge sign for selected $|Z| \geq 2$ events.

Heavy nuclei were identified in the range $3 \leq Z \leq 8$ with a good charge separation capability. In this preliminary configuration of the detector, the detection efficiency for $Z \geq 7$ was low. The following discussion is therefore limited to $2 \leq Z \leq 6$, where $1.16 \times 10^5$ nuclei were identified.

Since no antimatter nuclei were observed, we can only establish an upper limit on their flux.

For each nucleus with charge $Z$, the measured rigidity spectrum was corrected for the detector resolution and efficiency as a function of the measured, $\mathrm{R}_m$, and incident, R, rigidity. The detection efficiencies including the rigidity resolution function, $f(\mathrm{R}, \mathrm{R}_m)$, were evaluated through complete Monte Carlo simulation using the GEANT Monte Carlo package (Brun et al. , 1987). In addition, nuclear interactions

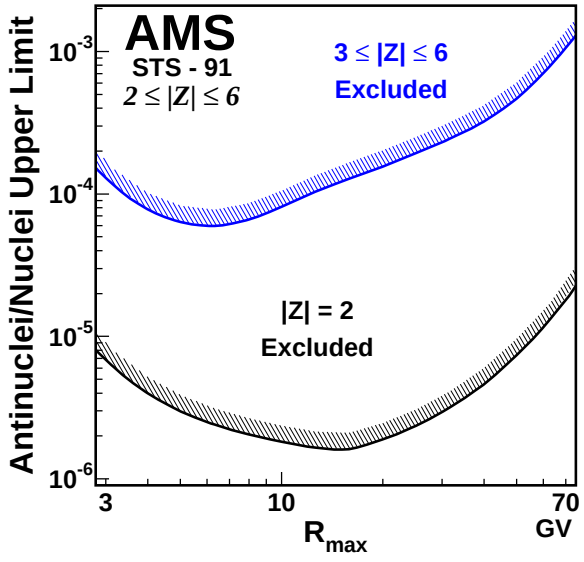


**Fig. 5.** Upper limits on the relative flux of antimatter to matter, at the 95% confidence level, as a function of the rigidity interval $\mathrm{R} = 1.6\,\mathrm{GV}$ to $\mathrm{R}_{max}$. These results are independent of the incident antimatter spectra.

were simulated using the RQMD package (Sorge , 1995). The incident rigidity spectra, $dN'/d\mathrm{R}$ were extracted from the measured spectra, $dN'/d\mathrm{R}_m$, by numerical deconvolution of $dN'/d\mathrm{R}_m = \int (dN'/d\mathrm{R}) \times f(\mathrm{R},\mathrm{R}_m) d\mathrm{R}$ (Kondor , 1983). To obtain the detector efficiencies for each antinucleus species, $\epsilon_{\overline{Z}}(\mathrm{R})$, a small correction was applied to the efficiencies for the corresponding nucleus, $\epsilon_Z(\mathrm{R})$, based on the estimated difference in absorption cross sections (Moiseev and Ormes , 1997).

Letting $N_Z(\mathrm{R}_i)$ be the number of incident nuclei in the rigidity bin $(\mathrm{R}_i, \mathrm{R}_i + \Delta\mathrm{R})$ and $N'_Z(\mathrm{R}_i)$ be the number of measured $Z$ in the same rigidity bin after correction for the detector resolution, then $N'_Z(\mathrm{R}_i) = \epsilon_Z(\mathrm{R}_i) N_Z(\mathrm{R}_i)$, where $\epsilon_Z(\mathrm{R}_i)$ is the detection efficiency in this bin, and similarly for antinuclei. Over the rigidity interval studied no $\overline{Z}$ were found, $N'_{\overline{Z}}(\mathrm{R}_i) = 0$ for each $i$. At the 95 % confidence level this is taken to be less than 3 and the differential upper limit for the flux ratio for each nucleus is given by:

$$\frac{N_{\overline{Z}}(\mathrm{R}_i)}{N_Z(\mathrm{R}_i)} < \frac{3/\epsilon_{\overline{Z}}(\mathrm{R}_i)}{N'_Z(\mathrm{R}_i)/\epsilon_Z(\mathrm{R}_i)} \,. \qquad (1)$$

We can now compute upper limits for the antimatter to matter flux ratio as follows:

(i) Here we assume that the incident antimatter ($\overline{\mathrm{He}}$ or $\overline{Z}$) rigidity spectrum has the same shape as the corresponding He or $Z$ spectrum over the range $1 < \mathrm{R} < 140\,\mathrm{GV}$. If we further assume that the charge composition of antimatter has the same shape as the corresponding matter spectrum over the range $2 \le Z \le 6$, we can sum equation (1) over all rigidity bins and charges. This yields a limit of:

$$\frac{N_{\overline{\mathrm{He}}}}{N_{\mathrm{He}}} < 1.1 \times 10^{-6} \quad \text{and} \quad \frac{N_{\overline{\mathcal{N}}}}{N_{\mathcal{N}}} < 2.9 \times 10^{-5} \,. (2)$$

(ii) For a conservative upper limit, which does neither depend on the assumed antimatter rigidity spectrum nor on the assumed antimatter charge composition, events for all $Z$ are added in intervals from $\mathrm{R}_{min} = 1.6\,\mathrm{GV}$ up to a variable $\mathrm{R}_{max}$. For each such interval the minimum value of the efficiency $\epsilon_{\overline{Z}}$ is taken for all rigidity bins and for all charges, yielding

$$\frac{N_{\overline{\mathcal{N}}}}{N_{\mathcal{N}}} < \frac{3/\epsilon^{min}_{\overline{Z}}(\mathrm{R}_{min},\mathrm{R}_{max};\mathcal{N})}{\sum_Z \sum_i N'_Z(\mathrm{R}_i)/\epsilon_Z(\mathrm{R}_i)} \,, \qquad (3)$$

where $\mathrm{R}_i = (\mathrm{R}_{min},\mathrm{R}_{max})$ and $\mathcal{N}$ stands for He or heavy nuclei. These results are shown in Fig. 5 as a function of $\mathrm{R}_{max}$ for $|Z| = 2$ and $3 \le Z \le 6$.

In conclusion, we found no antimatter nuclei at any rigidity. Up to rigidities of 140 GV, $2.86 \times 10^6$ helium nuclei and $1.65 \times 10^5$ heavier nuclei were measured. Assuming the antimatter rigidity spectrum to have the same shape as the matter spectrum, an upper limit at the 95 % confidence level on the relative flux of antihelium to helium of $1.1 \times 10^{-6}$ and of heavier antinuclei to nuclei ($3 \le Z \le 6$) of $2.9 \times 10^{-5}$ was obtained. This result is an improvement in both sensitivity and rigidity range over previous measurements (Saeki et al. , 1998). This flight has shown that the completed AMS on the International Space Station will provide many orders of magnitude of improvement in the sensitivity to search for antimatter.

## References

S. Ahlen et al., Nucl. Inst. Meth. A 350 (1994) 351
J. Alcaraz et al., Phys. Lett. B 461 (1999) 387-396
R. Brun et al.,"GEANT 3", CERN DD/EFJ84-1 (revised), 9/1987
A. Kondor, Nucl. Inst. Meth. A 216 (1983) 177
A. Moiseev and J. Ormes, Astropart. Phys.6 (1997) 379
T. Saeki et al., Phys. Lett. B 422 (1998) 319
H. Sorge, Phys. Rev. C52 (1995) 3291
G. Viertel and M. Capell, Nucl. Inst. Meth. A 419 (1998) 295